Extending the Photon Mapping Method
for Realistic Rendering of Hot Gaseous Fluids

Byungkwon Kang[†], Insung Ihm[†], Chandrajit Bajaj[‡]

[†] Department of Computer Science
Sogang University
Seoul, Korea

[‡] Department of Computer Sciences
University of Texas at Austin
Austin, Texas, U.S.A.

Abstract

With the increased sophistication and use of heated gas, fire, and explosion simulations in computer graphics applications, there is a corresponding impetus to improve the visual realism in the rendering of such simulated phenomena. In visualizing these turbulent fluids, an appropriate incorporation of their incandescent properties into the rendering significantly enhances the realism of visual effects. In this paper, we effectively synthesize the light emission phenomena of hot gaseous fluids by extending the photon mapping global illumination method. In particular, we add two new photon maps to capture the thermal radiation effects. First, we define an *emission* photon map to store the photons emitted within hot gaseous fluids. Second, we utilize additional *flash* and *flash reflection* photon maps, which are effective in creating a visual effect of light that intensively and instantly propagates outside hot gaseous fluids, visually capturing shock waves. Our current technique, while based on the theory of blackbody radiation, is parameterized to enable an animator to generate a wide range of visual effects with fairly intuitive user control. We demonstrate the effectiveness of our new rendering technique and user-controlled generation of visual effects with several example pictures and animations.

Keywords: Rendering, gaseous fluids, incandescence, blackbody radiation, photon mapping, physically based fluid animation.

1 Introduction

Among a variety of natural phenomena, hot gaseous fluids, ranging from simple smoke and gas to fire flames and explosions, abound in the real world, and are often indispensable ingredients in the production of computer animations. Many simulation techniques for such fluids have long been developed in the computer graphics community for the purpose of effective visual applications. In particular, recent research efforts to exploit numerical simulation methods in computational fluid dynamics have proved very successful. As a result, diverse physically based fluid animation techniques are now routinely applied to create realistic visual effects of hot gaseous fluids.

While realistic rendering of simulated fluids is an essential part of a fluid animation process, researchers have focused mainly on generating appealing motions and controlling their shapes. Physically based simulation techniques generally produce their results in the form of volumetric datasets, describing physical properties of gaseous fluids, such as density, temperature, pressure, and velocity. Obviously, the most decisive attribute that affects the appearance of fluids in the rendered images is their density. However, the temperature property also becomes important when hot gaseous fluids that give out light are to be rendered. Although volume rendering has been studied rigorously, primarily for visualizing the density field, only a few studies of computer animation have seriously dealt with

the effective rendering of physically simulated hot gaseous fluids that emit thermal radiation.

Handpicked color maps that convert temperature to emitted colors have often been used to generate incandescent effects. For example, simulated flames and explosion were visualized using color maps, obtained from reference images [1, 2, 3], where Lamorlette and Foster [1] approximated the flame's incandescence using a user-controlled energy function.

More physically based fluid rendering methods have also been presented, in which the theories of blackbody radiation and light transport in participating media are exploited in an attempt to simulate the thermal radiance precisely. Stam and Fiume [4] evaluated the intensity of light traveling along a ray using a radiative light transport equation that described the scattering, absorption, and emission properties of gaseous fluids. In this work, Planck's spectral radiance function of a blackbody was employed to estimate the light emission from the temperature field that evolves under an advection–diffusion-type model. Yngve et al. [5] also applied this function to select the radiant color of particles that simulate an explosion. Nguyen et al. [6] computed the incandescent color of fire by integrating Planck's function, and then transforming the raw color for a chromatic adaptation. The final rendering of fire used a stochastic adaptive ray-marching algorithm to solve the light transport equation. Rasmussen et al. [7] considered the particles simulated for a large-scale explosion as blackbodies; their temperatures were mapped to radiant colors using a user-controlled map. Light scattering within the exploding fluid was modeled through a simple diffusion process, similar to that in [4], assuming that the fluid was a high albedo medium.

This work continues these efforts to achieve a high-quality rendering from physically simulated fluid data. The theory of blackbody radiation is exploited in our photon mapping scheme to realistically synthesize the light emission phenomena of hot gaseous fluids. Photon mapping is a Monte Carlo-based algorithm that has proved very efficient in rendering various global illumination effects [8]. In particular, scenes with participating media are easily rendered by extending the Monte Carlo ray tracer using a volume photon map [9].

In this paper, we add two more photon maps to represent the thermal radiation effect. First, a photon map called the *emission* photon map is defined to store the photons emitted within hot gaseous fluids. Secondly, we employ additional photon maps called the *flash* and *flash reflection* photon maps, which are useful for producing a visual effect of light that intensively and instantly propagates outside hot gaseous fluids. Compared to the emission photon map, the flash photon map may not appear physically based, but is shown to be very effective in creating a flash-like effect that is difficult to simulate or render using existing techniques.

Our extensions can be added quite simply to a photon mapping-based ray tracer, and are flexible enough to enable an animator to create a wide range of visual effects related to the thermal radiation of hot gaseous fluids. In implementation, the emission and flash reflection photon maps are easily incorporated into the volume and caustics photon maps, respectively, while we need another map to store the flash photons. In extending the existing rendering method, a new set of physically motivated parameters is introduced. Using examples, we show how they can be manipulated effectively to adjust the thermal radiation effects.

2 Related work

The research efforts in computer graphics that attempt to solve the full three-dimensional Navier–Stokes equations have allowed very realistic simulations of smoke and gas [10, 11, 12] to be carried out. Ihm et al. [13] recently extended these models, based on the theory of chemical reaction, to handle reactive gaseous fluids. In addition to the generation of appealing motions of gaseous fluids, several interesting methods for modeling their shapes have been developed [14, 15, 16]. Numerous studies have also been directed at developing practical techniques for modeling realistic explosions using various physically based and/or ad hoc fluid models [17, 18, 5, 2, 7]. Fire and flame are dramatic special effects frequently employed in fluid animation, and have been modeled in several previous studies including [4, 19, 6, 1, 20, 21].

Most of these studies involved hot gaseous fluids that may give out visible light and other electromagnetic radiation as a consequence of their temperature. The laws basic to the thermal light sources can be explained best by the theory of blackbody radiation [22], which is briefly introduced before. The photons emitted within gaseous fluids are absorbed and scattered as they propagate through the participating media, where this light transport phenomenon is described by the radiative transport equation [23, 24]. Interested readers are referred to [25, 26, 27] for extensive lists of existing global illumination methods for participating media.

The behavior of light in participating media is well simulated by the photon mapping method, which is a two-pass global illumination technique. In the first pass, the relevant photon map structures are built by emitting photons from light sources and tracing them through the scene. Then the information in the photon maps is used during the rendering pass for an efficient Monte Carlo estimation of indirect illuminations. For more details on photon mapping, refer to [8].

3 Preliminaries: incandescence and blackbody radiation

Incandescent substances like the sun, candle flames, and tungsten lamp filaments, give out light when heated. Physically, the phenomenon of incandescence is explained by the theory of thermal radiation, which studies the principles of heat transfer caused by electromagnetic waves or photons [22]. A blackbody is an idealized body that is both a perfect absorber and emitter of radiation. It absorbs all the radiation that falls onto it, and then gives off all that energy as radiation in the form of electromagnetic waves. No body at a given temperature can emit more radiation than a blackbody at the same temperature. While it is a hypothetical body, it serves as a standard to which the radiative properties of real bodies may be compared.

Many physicists have attempted to find radiation laws that can measure an amount of radiation. The primary principle governing blackbody radiation is Planck's law, which formulates thermal radiation in terms of the spectral emissive power distribution $E(\lambda, T)$. It gives the intensity radiated by a blackbody as a function of wavelength at a given temperature:

$$E(\lambda, T) \quad = \frac{2hc^2}{\lambda^5} \frac{1}{e^{hc/\lambda kT}-1},$$

where the constants h ($\approx 6.6237 \cdot 10^{-34}$ Js), k ($\approx 1.380 \cdot 10^{-23}$ JK^{-1}), and c ($\approx 2.9979 \cdot 10^8$ ms^{-1}) denote Planck's constant, Boltzmann's constant, and the speed of light, respectively (see Figure 1). The total energy emitted at all wavelengths from a blackbody is obtained by integrating the spectral distribution function. The Stefan–Boltzmann law indicates that the total energy flux Φ emitted from a blackbody is directly proportional to the fourth power of the temperature:

$$\Phi(T) \quad = \quad \pi \int_0^\infty E(\lambda, T) \, d\lambda = \sigma T^4,$$

where σ ($\approx 5.6696 \cdot 10^{-8}$ $Wm^{-2}K^{-4}$) is called the Stefan–Boltzmann constant.
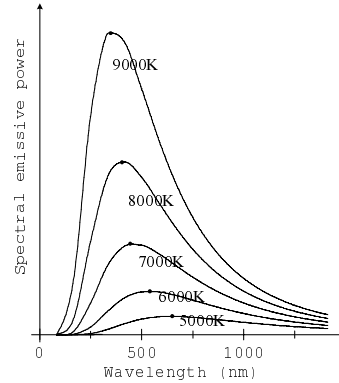

Figure 1: Planck's spectral radiation distribution function $E(\lambda, T)$.

The spectral radiation effectively extends over a continuous range of wavelengths, emitting more energy at all wavelengths as the temperature increases. As revealed in the graph of the spectral distribution function in Figure 1, the peak wavelength of the blackbody radiation shifts to shorter wavelengths at higher temperatures. Wien's displacement law states that there is an inverse relation between the wavelength λ_{max} (in m) of the maximum intensity and the temperature T (in K):

$$\lambda_{max} = \frac{0.002898}{T}. \tag{1}$$

Basically, the hotter a blackbody is, the shorter the wavelengths at which it emits radiation. Note that all objects emit electromagnetic radiation. Even an object at room temperature emits some radiation. However, because all but a negligible amount of the emitted energy lies in the infrared in the electromagnetic spectrum, the radiation is invisible, and is only detectable as warmth. When the temperature of the body increases to about 1000K, the range of wavelengths emitted enters the red end of the visible spectrum and the body becomes red hot. As the body heats up more, the peak wavelength continues to decrease, changing its color to orange, then yellow to white, and finally to blue-white.

4 Extending the photon mapping method for light-emitting gaseous fluids

In this section, we explain how the photon mapping method is extended to include thermal radiation effects for physically simulated gaseous fluids. In the original photon mapping method, a global photon map is used to represent all illuminations in the scene, including direct illumination and caustics. As well as being represented in the global photon map, caustics are also treated specially by using a caustics photon map for efficient highlight computations. As well, a volume photon map is employed to express the light's interaction with participating media. The new photon maps defined here have the same structure as these maps, and hence can be easily incorporated in photon map-based ray tracers.

4.1 The emission photon map

To simulate the thermal radiation emitted from hot gaseous fluid, we construct a photon map called the *emission photon map*. In our scheme, the fluid is assumed to be filled with random hypothetical blackbody particles that send out thermal energy isotropically as photons. In the photon tracing phase, the photons that are emitted and then propagated in the fluid are represented in this photon map. In the following rendering step, the information in the map is integrated

over the volume of the participating media to produce a realistic thermal radiation effect.

4.1.1 Construction of the emission photon map

Consider a volume dataset that stores the fluid's density and temperature. The first step in building the emission photon map is to determine the amount of radiation energy emitted at each voxel. For the time being, we consider only visible light with wavelengths ranging from $380nm$ to $780nm$. Then, the total emissive power of a voxel is evaluated by integrating the spectral intensity over the range $[\lambda_{min}, \lambda_{max}] = [380, 780]$:

$$\Phi_{tep}(T, \lambda_{min}, \lambda_{max}) = \pi \int_{\lambda_{min}}^{\lambda_{max}} E(\lambda, T) \, d\lambda, \tag{2}$$

where T is the temperature of the voxel. The spectral intensity function is not integrable analytically, hence an appropriate numerical quadrature method must be applied. In this work, we evaluate the integral using a fast-converging closed-form formula, expressed in terms of polylogarithm functions [28].

The quantity $\Phi_{tep}(T, \lambda_{min}, \lambda_{max})$ indicates the total power of visible light emitted in the corresponding cell region. This radiation energy is uniformly subdivided among the randomly distributed blackbody particles in the cell, which in turn send out photons isotropically, transporting each fraction of the thermal radiation energy. To simulate this process stochastically, we generate photons using Monte Carlo sampling as follows: first, the number n_{ep} of photons created in the cell is decided by rescaling the total power as $n_{ep} = f_{nep}(\Phi_{tep}(T, \lambda_{min}, \lambda_{max}))$, where $f_{nep}(\cdot)$ is a global function that approximately controls the total number of photons to be stored in the emission photon map. Then, the initial positions and shooting directions of n_{ep} photons are generated using a uniformly distributed random function.

In addition, the powers and colors of the emitted photons are also determined stochastically. As we suppose that the total power $\Phi_{tep}(T, \lambda_{min}, \lambda_{max})$ is evenly distributed among the photons produced in the cell, all the photons are assumed to have the identical power

$\Phi_{ep} = \frac{\Phi_{tep}(T, \lambda_{min}, \lambda_{max})}{n_{ep}}$. On the other hand, their colors are computed in a way that reflects the radiant property of blackbody that is represented by Planck's spectral radiation distribution function $E(\lambda, T)$ (see Figure 1 again). For this, we perform importance sampling of $E(\lambda, T)$ over $[\lambda_{min}, \lambda_{max}]$ to obtain n_{ep} wavelengths. Then the respective colors C_{ep} of the photons are computed from the sampled wavelengths through the color spectrum. In this way, the thermal radiation phenomenon in each cell is stochastically represented, based on the theory of blackbody radiation. Note that the simulated temperature T decides the photon generation process.
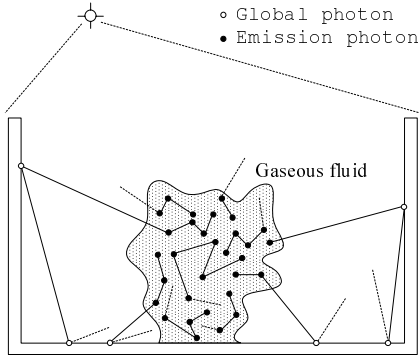

Figure 2: The emission photon map.

Once the number of photons and their geometric and spectral properties are determined, they start to travel through the gaseous fluid, the participating medium, based on the light transport model (see Figure 2). The photons are stored in the emission photon map every time they interact with the fluid. As they leave the medium, they turn into global photons. The emission photon map is basically the same as the volume photon map [9], except that photons are created inside the volume, so the extension can be easily incorporated in a conventional photon mapping-based ray tracer.

4.1.2 Controlling the rendering effects

While the temperature T in the spectral intensity function denotes absolute temperatures in the Kelvin scale, the simulated temperature values often do not accord with the scale, making it necessary to rescale the temperature space. This adaptation procedure offers a useful mechanism that allows an animator to control the overall brightness and hues of the incandescence, because the temperature distribution greatly affects the color of thermal radiation.

For instance, suppose that an animator wishes to make the radiant color of a simulated fluid appear roughly in the spectral range from red to yellow. An intuitive technique is to map the simulated temperatures to an interval with its upper limit matched roughly to the yellow color through Wien's displacement law. That is, the color temperature with a peak wavelength in the spectral distribution curve corresponding to yellow light with $\lambda_{yellow} = 570nm$, can be obtained using Eq (1) as $T_{yellow} = \frac{0.002898}{\lambda_{yellow}}$. By transforming the raw temperatures to the space $[0, T_{yellow}]$, the resulting incandescent color can be effectively restricted to the desired color spectrum.

It is also possible to control the radiation color by adjusting the integral domain $[\lambda_{min}, \lambda_{max}]$ in Eq (2). Because Planck's radiation function is importance-sampled in the wavelength domain during the photon generation phase, modifying the interval directly influences the color tone of emitted photons. For example, instead of using the entire range $[380, 780]$ for visible light, the reddish color in the radiation can be eliminated by appropriately lowering the upper bound. Our experiments indicate that it is possible to adjust the tone of emitted light with fine control.

Lastly, the scattering and absorption coefficients σ_s and σ_a of the participating media (and its scattering albedo $\Lambda = \frac{\sigma_s}{\sigma_s + \sigma_a}$) may be used to adjust the general brightness and the extent to which the thermal radiation spreads out, as will be shown later.

4.2 The flash photon map

In computer graphics, a flash effect is often used to synthesize impressive rendering images. It includes all phenomena regarding a sudden burst of light or of something shiny or bright. A good example in fluid animation is a bright flash that is released instantly by the fireball that follows a big explosion and spreads over a wide area, diminishing with distance. Although this kind of flash is, in fact, a thermal radiation phenomenon caused by a sudden, intensive release of high energy, it is quite difficult to physically simulate and render it because of its numerical instabil-

ity. Such a flash effect can be easily generated in the photon mapping scheme by introducing another photon map called the *flash photon map*. Compared to the emission photon map, this extension may not appear physically based, but is shown to be very effective in creating a variety of flash-like effects with user control.

4.2.1 Construction of the flash photon map

In the proposed scheme, the flash phenomenon is modeled using a collection of imaginary *flash particles* that are cast outwards from the gaseous fluid. Like the emission photons, they are generated within the gaseous fluid, but an energy value is assigned to each one according to the total emissive power. They propagate through the medium and, unless they are extinguished, in the air, continuously consume their energies. The flash particles are similar to the emission photons in that they are scattered as they propagate through the medium. However, each flash particle loses its own energy as it travels independently, and becomes extinct only when it spends all energy. When the particle leaves the participating medium alive, it continues to follow a straight line in the air.
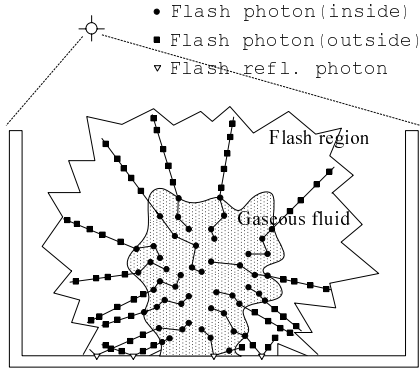

Figure 3: The flash photon map.

During its traversal, each flash particle generates a series of *flash photons* along its path (see Figure 3). Inside the participating medium, a photon is stored in the flash photon map every time the particle is scattered. When the particle leaves the medium, the length of the straight propagation is estimated based upon the remaining energy, and the path in the air is stochastically sampled using a user-controlled density

parameter δ_{fp}. Contrary to the volume or emission photon that becomes a global photon when it leaves the medium, the flash particle keeps producing flash photons at the sampling positions, and storing them in the flash photon map.

4.2.2 Controlling the rendering effects

In creating a flash effect, it is important to be able to control its strength and extent intuitively. One of the most influential factors is the energy ϵ_{fp} initially assigned to a flash particle. We assume that all flash particles generated in a given cell have the same energy, computed as a function of the total emissive power $\epsilon_{fp} = f_{efp}(\Phi_{tep}(T, \lambda_{min}, \lambda_{max}))$, where the empirical function $f_{efp}(\cdot)$ enables an animator to adjust the overall strength of flash light. Combined with this function, a user-controlled rate γ_{fp} of the decrease in energy per unit length can control how far the flash light reaches.

The number n_{fp} of flash particles starting from the cell is set to $n_{fp} = \frac{\Phi_{tep}(T, \lambda_{min}, \lambda_{max})}{\epsilon_{fp}}$. Unlike the initial energy ϵ_{fp} and the number of particles n_{fp} that are computed cell by cell, reflecting each cell's temperature, the power and color (Φ_{fp}, C_{fp}) of the generated flash photons are uniquely chosen by the animator.

The seeding positions and initial directions of the particles are also selected stochastically. Unlike the emission photons that are always sent out isotropically, we allow the flash particles to be emitted within a cone, defined by a direction d_{cone} and a cutoff angle α_{cone}, to make the resulting flash more directional. For example, by controlling the cutoff angle α_{cone} aligned along the negative gradient direction of the temperature field $d_{cone} = -\nabla T$, an animator can adjust the sharpness of a flash. In scattering the flash particles, we also find that a forward scattering, chosen through a positive g value in the Henyey–Greenstein phase function [29] helps create a harsher flash effect. Lastly, the density δ_{fp} at which the particle's path is sampled in the air affects the brightness and smoothness of the flash light outside the medium.

4.2.3 Extending the ray tracer

To use the flash photon map, the Monte Carlo ray tracer must be modified slightly. When a ray

intersects with a flash region that includes the participating medium, we perform ray marching to evaluate, via the integration of the volume rendering equation, all the contributions from the volume, the emission, and the flash photon maps. At each sampling point x, the radiance $C_{ve}(x)$ stemming from the volume and the emission maps, if x is in the medium, is first estimated by measuring their photon density, as explained by Jensen [8]. The opacity of the medium is also evaluated as $\alpha_{ve}(x) = 1 - e^{-\sigma(x)\Delta x}$.

In addition to these, the density of the flash photons is evaluated to reflect the contribution from the flash photons appropriately. A good value is $\alpha_f(x) = \alpha_f^{max} \cdot \frac{N(x)}{N_{max}}$ with user-controlled parameters α_f^{max} and N_{max}. α_f^{max} is a parameter that adjusts the maximum opacity of the flash light, N_{max} is the maximum number of flash photons searched inside a spherical volume centered at x, and $N(x)$ is the actual number of flash photons found. Then the color and opacity $(C(x), \alpha(x))$ at the sampling point x are obtained by combining these figures as $\alpha(x) = \alpha_{ve}(x) + \alpha_f(x)$ and $\alpha(x)C(x) = \alpha_{ve}(x)C_{ve}(x) + \alpha_f(x)\Phi_{fp}C_{fp}$, where Φ_{fp} and C_{fp} are, again, the flash photon's power and color, respectively. Notice that the smoothness of the flash effect can be controlled by N_{max} and the radius r_{sp} of the sphere used in estimating the local photon density.

4.2.4 The flash reflection photon map

Sometimes, a traversing flash particle hits a surface before it dies, implying that a bright flash of light is directly shed on the surface. This intensive illumination can be simulated more effectively by employing another photon map, called the *flash reflection photon map*. When a flash particle hits a surface, a flash reflection photon is stored in the map before it is reflected. In the rendering phase, the new map is treated like the caustics photon map, as both maps are intended to depict an intense highlight effect. We observe that a simple Gaussian filter, for instance, one proposed by Pavicic [30], works well for emphasizing the flash light on the surface.
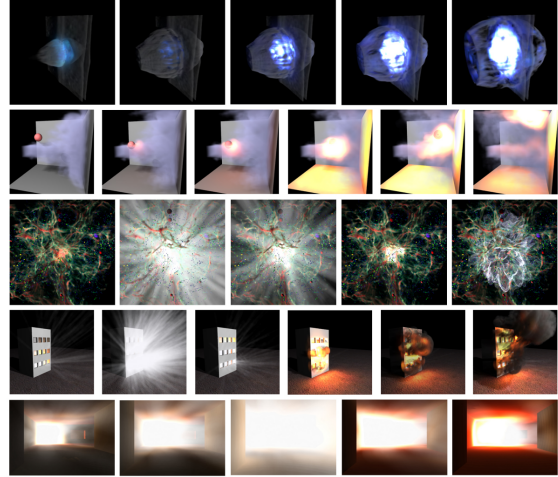

Figure 4: Tested animation scenes.

5 Rendering results

We have fully implemented our rendering technique as a photon map based Monte Carlo ray tracer and present several example pictures and animations, demonstrating rendering quality and parameter flexibility. Figure 4 shows several scenes capturing the thermal radiation effects generated by various hot gaseous fluids. The images in the first two rows were rendered with the emission photon map only, while the flash photon map was added for flash-like effects in the remaining images.

Our experiments with several physically-simulated datasets indicate that the various control parameters, explained in the paper, allow quite intuitive controls in tracing and rendering the emission and the flash photons. For example, the scene in the first row of Figure 4 was created using a restricted range $[\lambda_{min}, \lambda_{max}] = [380, 550]$ in an attempt to emphasize a blueish color, while quite different color tones of the thermal radiation were achieved with different ranges. Figure 5(a) was simulated using the entire visible spectral range $[380, 780]$. On the other hand, the images in (b) were produced with another one $[570, 780]$, covering the red to yellow range. These three images also suggest that the scattering albedo Λ is a useful parameter that can control the overall radiation effect. As shown in the figures, the gaseous fluid becomes brighter as Λ increases from 0.3 by 0.2 (from left to right).

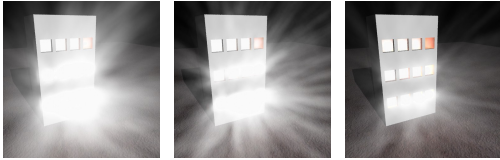Visually interesting flash-like effects can be
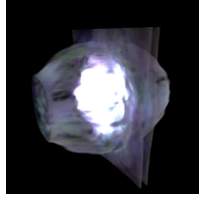
(a) Entire spectrum
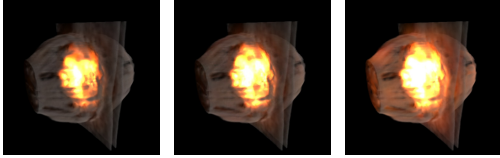
(b) Λ = 0.3, 0.5, and 0.7 (from left to right)

Figure 5: Adjustment of emission effects.

(a) $(r_{sp}, N_{max}) = (15.0, 700), (8.0, 300),$ and $(8.0, 700)$ (from left to right)

(b) Before and after the application of the flash reflection photon map

Figure 6: Adjustment of flash effects.

also created with fairly intuitive user control, as shown in Figure 6. The images in (a) imply that the radiance estimation parameters r_{sp} and N_{max} are also quite useful for controlling the smoothness of the flash effect. As shown in the three images, increasing the radius r_{sp} of the sphere used for the volume radiance estimate and the maximum number N_{max} of the nearest flash photons sought, makes the flash light smoother. Figure 6(b) compares the two rendered images generated respectively without and with the use of the flash reflection photon map described before. As the rendering result shows, the direct illumination caused by the flash light becomes more evident through the flash refection photon map.

In Table 1, information about the sizes of created photon maps along with the computation times required for building the photon map

Figure 7: Image samples obtained by varying the number of flash photons.

structures and rendering the frames is listed. The statistics were compiled while rendering the respective images of resolution 500×500 shown in the third and fourth rows of Figure 4. Here, surface denotes the number of the regular photons that are stored on the surfaces of polygonal models. volume indicates the size of the volume photon map that includes the emission photons. flash represents the number of stored flash photons, whereas flash-refl shows that of the flash reflection photon map that is implemented as a caustics photon map. p-tracing shows the time for building all the photon map structures. On the other hand, rendering represents the rendering time required to render the scene with one ray sample per pixel, measured on a PC equipped with 2.8GHz Intel Pentium 4 CPU. One sample per pixel was enough for the scene in the third row, while we fired six jittered rays per pixel in the next scene since the simulation grid size is too small compared to the image resolution.

Notice that several rendering parameters greatly affect the rendering quality and time. For instance, Figure 7 illustrates three image samples that were created by varying the number of flash photons. In this test, 263,753, 537,102, and 1,063,847 flash photons were created during rendering these images (from left to right), while other rendering parameters were fixed. As more flash photons are produced, the time for building the photon maps increases from 237.4 seconds, 426.1 seconds, and to 615.8 seconds, respectively, whereas the ray sampling time is rather insensitive to the number of the photons.

Finally, to help judge the realism of our results, Figure 8 shows an interesting image recently released by National Aeronautics and Space Administration (NASA) [31]. This image, named *Gone in a flash*, shows an actual flash-like effect caused by the initial ejecta that resulted when NASA's Deep Impact probe collided with comet Tempel 1. Compare this with

(a) Statistics for the images in the third row of Figure 4 (simulation grid size: $255 \times 255 \times 255$)

frame no.	surface	volume	flash	flash-refl	p-tracing (sec.)	rendering (sec.)
4	0	1,829	0	0	4.5	815.5
5	0	48,795	53,986	0	59.1	2145.9
14	0	21,054	14,899	0	25.8	1655.9
17	0	8,425	0	0	12.4	821.9
50	0	6	0	0	0.03	989.8

(b) Statistics for the images in the fourth row of Figure 4 (simulation grid size: $120 \times 100 \times 80$)

frame no.	surface	volume	flash	flash-refl	p-tracing (sec.)	rendering (sec.)
3	48,113	23,220	15,953	12,122	50.7	141.1
4	1,914,608	2,112,280	606,007	495,571	1,317.5	830.7
6	654,730	553,213	181,252	28,710	441.1	346.6
13	575,815	589,210	3,717	2,774	339.0	328.9
16	535,118	471,538	5,948	2,559	581.1	552.1
20	545,121	449,038	7,389	680	375.4	407.2

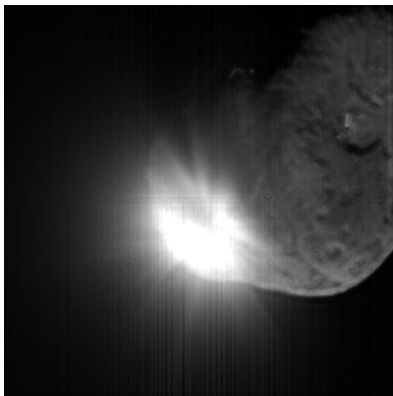Table 1: Rendering statistics for two sample scenes.

Figure 8: The image *Gone in a flash* (Courtesy of NASA/JPL-Caltech/UMD).

our rendered images.

6 Conclusions

Gas hydrodynamic simulation techniques routinely generate various additional time varying physical quantities such as gas velocity and pressure, besides the evolving gas density and temperature. A natural extension to our current method, where we exploited the light emitting effects of a combination of gas density and temperature, is to capture enhanced visual effects dependent on these additional variables. For ex-

ample, close to fixed or moving structures inside the dynamic gaseous fluid, one could render additional photons generated due to the created vortices to enhance the overall photo-realism.

Acknowledgements

References

[1] A. Lamorlette and N. Foster. Structural modeling of flames for a production environment. *ACM Transactions on Graphics (ACM SIGGRAPH 2002)*, 21(3):729–735, 2002.

[2] B. Feldman, J. O'Brien, and O. Arikan. Animating suspended particle explosions. *ACM Transactions on Graphics (ACM SIGGRAPH 2003)*, 22(3):708–715, 2003.

[3] F. Pighin, J. M. Cohen, and M. Shah. Modeling and editing flows using advected radial basis functions. In *Proc. of Eurographics/ACM*

SIGGRAPH Symposium on Computer Animation 2004, pages 223–232, 2004.

[4] J. Stam and E. Fiume. Depicting fire and other gaseous phenomena using diffusion processes. In *Proc. of ACM SIGGRAPH 1995*, pages 129–136, 1995.

[5] G. Yngve, J. O'Brien, and J. Hodgins. Animating explosions. In *Proc. of ACM SIGGRAPH 2000*, pages 29–36, 2000.

[6] D. Nguyen, R. Fedkiw, and H. Jensen. Physically based modeling and animation of fire. *ACM Transactions on Graphics (ACM SIGGRAPH 2002)*, 21(3):721–728, 2002.

[7] N. Rasmussen, D. Nguyen, W. Geiger, and R. Fedkiw. Smoke simulation for large scale phenomena. *ACM Transactions on Graphics (ACM SIGGRAPH 2003)*, 22(3):703–707, 2003.

[8] H. W. Jensen. *Realistic Image Synthesis Using Photon Mapping*. A K Peters, Ltd, ISBN 1-56881-147-0, 2001.

[9] H. W. Jensen and P. H. Christensen. Efficient simulation of light transport in scenes with participating media using photon maps. In *Proc. of ACM SIGGRAPH 1998*, pages 311–320, 1998.

[10] N. Foster and D. Metaxas. Modeling the motion of a hot, turbulent gas. In *Proc. of ACM SIGGRAPH 1997*, pages 181–188, 1997.

[11] J. Stam. Stable fluids. In *Proc. of ACM SIGGRAPH 1999*, pages 121–128, 1999.

[12] R. Fedkiw, J. Stam, and H. Jensen. Visual simulation of smoke. In *Proc. of ACM SIGGRAPH 2001*, pages 23–30, 2001.

[13] I. Ihm, B. Kang, and D. Cha. Animation of reactive gaseous fluids through chemical kinetics. In *Proc. of Eurographics/ACM SIGGRAPH Symposium on Computer Animation 2004*, pages 203–212, 2004.

[14] A. Treuille, A. McNamara, Z. Popović, and J. Stam. Keyframe control of smoke simulations. *ACM Transactions on Graphics (ACM SIGGRAPH 2003)*, 22(3):716–723, 2003.

[15] A. McNamara, A. Treuille, Z. Popović, and J. Stam. Fluid control using the adjoint method. *ACM Transactions on Graphics (ACM SIGGRAPH 2004)*, 23(3):449–456, 2004.

[16] R. Fattal and D. Lischinski. Target-driven smoke animation. *ACM Transactions on Graphics (ACM SIGGRAPH 2004)*, 23(3):441–448, 2004.

[17] M. Neff and E. Fiume. A visual model for blast waves and fracture. In *Proc. of Graphics Interface 1999*, pages 193–202, 1999.

[18] O. Mazarak, C. Martins, and J. Amanatides. Animating exploding objects. In *Proc. of Graphics Interface 1999*, pages 211–218, 1999.

[19] P. Beaudoin, S. Paquet, and P. Poulin. Realistic and controllable fire simulation. In *Proc. of Graphics Interface 2001*, pages 159–166, 2001.

[20] X. Wei, W. Li, K. Mueller, and A. Kaufman. Simulating fire with texture splats. In *Proc. of IEEE Visualization 2002*, pages 227–234, 2002.

[21] S. Hasinoff and K. Kutulakos. Photo-consistent 3D fire by flame-sheet decomposition. In *Proc. of the Ninth IEEE International Conference on Computer Vision*, pages 1184–1191, 2003.

[22] R. A. Serway, C. J. Moses, and C. A. Moyer. *Modern Physics*. Saunders College Publishing, ISBN 0-03-001547-2, 2nd edition, 1997.

[23] S. Chandrasekhar. *Radiative Transfer*. Dover, ISBN 0-48660-590-6, 1960.

[24] R. Siegel and J. Howell. *Thermal Radiation Heat Transfer*. Taylor & Francis Group, ISBN 1-56032-839-8, 4th edition, 2001.

[25] F. Perez-Cazorla, X. Pueyo, and F. Sillion. Global illumination techniques for the simulation of participating media. In *Proc. of the Eighth Eurographics Workshop on Rendering*, pages 309–320, 1997.

[26] M. Pharr and P. Hanrahan. Monte Carlo evaluation of non-linear scattering equations for subsurface reflection. In *Proc. of ACM SIGGRAPH 2000*, pages 75–84, 2000.

[27] S. Premože, M. Ashikhmin, R. Ramamoorthi, and S. Nayar. Practical rendering of multiple scattering effects in participating media. In *Proc. of the Eurographics Symposium on Rendering*, 2004.

[28] S. L. Moshier. Expressions for the integral of Planck's radiation formula. manuscript, 1999.

[29] L. G. Henyey and J. L. Greenstein. Diffuse radiation in the galaxy. *Astrophysics Journal*, 93:70–83, 1941.

[30] M. J. Pavicic. Convenient anti-aliasing filters that minimize bumpy sampling. In A. S. Glassner, editor, *Graphics Gems*, volume I, pages 144–146. Academic Press, ISBN 0-12-286165-5, 1990.

[31] NASA. *Deep Impact: A Smashing Success*. http://www.nasa.gov/mission_pages/deepimpact/main/index.html (Accessed: July 5, 2005), 2005.